Penetrator Formation Mechanisms during High-Frequency Electric Resistance Welding

The cause of a weld defect in steel pipe manufacture is identified

BY J.-H. CHOI, Y. S. CHANG, C.-M. KIM, J.-S. OH, AND Y.-S. KIM

ABSTRACT. In this study, welding phenomena involved in penetrator formation during high-frequency electric resistance welding were investigated. High-speed cinematography of the phenomena revealed that molten metal bridges, which formed between neighboring strip edges near the apex point, travel along a narrow gap toward the welding point at a speed much faster than that of the strip. Frequency of formation, travel distance, and speed of the bridge were affected mainly by the heat input power into the strip. Among the variables of the bridge traveling behavior, standard deviation of the travel distance appeared to have a strong relationship with defect density in weldments. Based on observation, a new mechanism of the penetrator formation during HF ERW process was proposed.

Introduction

The high-frequency electric resistance welding (HF ERW) process has been used extensively in manufacturing straight-seamed steel pipes. In this process, a strip is gradually formed into a circular tube shape through roll-forming stands, and its edges are supplied with high-frequency currents either by sliding contacts or by an inductor coil, as schematically illustrated in Fig. 1A. The high-frequency currents flow only through a thin surface layer of strip edge due to the skin and proximity effects (Ref. 1) and generate joule heat for forge welding at the upsetting roll stand. The penetration depth of 450 kHz currents in a steel heated to 800°C is, for example, approximately 0.8 mm (Ref. 2). This characteristic makes the process extremely energy efficient and its welding speed can be as high as 300 m/min. In addition, the weldment is relatively free of weld defects, especially the defects associated with weld solidification since molten metal mixed with oxides and impurities is squeezed out of the faying interface at the upsetting stage. Steel pipes produced via the HF ERW process, therefore, have been extensively used in critical applications requiring stringent weld qualities, such as line pipe and oil well casings.

There are, however, two major types of weld defects associated with the HF ERW process: the cold weld defect and the penetrator defect (Refs. 3, 4). The cold weld, an oxide inclusion in a form of continuous thin film at the weldment, has been observed when the heat input power into the strip is not large enough for adequate melting of the strip edges. The heat input power required for adequate melting is a function of various processing parameters that include strip thickness, strip speed, V angle, V length, and alignment of the strip edges. When only a very thin surface layer of the edge is melted with an insufficient heat input power, oxides on the surfaces may not be squeezed out along with the molten metal at the upsetting stage, leading to the cold weld defect. The oxides may be formed either during heating of the edges or during storage of the strip. On the other hand, the penetrator defect was reported to occur when heat input power is excessively large. The penetrator is a pancake-type morphology oxide inclusion that consists of Fe, Mn, and Si oxides (Ref. 5). The penetrator can be in a range of a few millimeters to a centimeter in size and critically affects the mechanical properties of pipes.

Several studies have been conducted to investigate the mechanism of penetrator formation. In their classical studies, Haga et al. (Refs. 6, 7) claimed that the penetrator is caused by backfilled molten metal mixed with the oxides into a narrow gap. The narrow, parallel gap between neighboring strip edges has been noted near the welding point during HF ERW (schematically shown in Fig. 1A). The narrow gap formation was attributed to the driving out of molten metal from strip edges by electromagnetic pinch force at the same rate as the approaching speed of the strip edges during welding. The approaching speed is determined by the strip speed and V angle (Ref. 6). In their studies, the narrow gap was reported to become unstable at high heat input powers, causing a short circuit at the apex point. When the short circuit occurs, the electromagnetic pinch force vanishes at the gap, and molten metal with the oxides refills the gap by capillary action. This backfilled metal mixed with the oxides was thought to cause the penetrator.

Penetrators, however, were observed even at heat input powers that are considered as a nominal welding condition (Ref. 8). In addition, several researchers have indicated that flashing or arcing occurs at the apex point during HF ERW (Ref. 9). At the instant of flashing, the electromagnetic pinch force that drives out the molten metal from the narrow gap should decrease dramatically since a significant fraction of current should be diverted through the flash. In this study, therefore, the phenomenon of penetrator formation was investigated in more detail by incorporating the effect of the flashing at the apex point. The HF ERW phenomena were investigated using a high-speed video camera and high-speed cinematography.

Experimental Procedures

High-frequency electric resistance welding was conducted using an 8-in. pipe mill (SeAh Steel Co. Ltd., Pohang, Korea) and an ERW simulator (POSCO, Pohang, Korea). Most of the experiments were conducted using the pipe mill equipped with a contact-type HF welding machine. An impeder with a water-cooled ferrite core was used to enhance efficiency of the welding machine. Welding speed tested was 18 m/min and strip thickness was 9.5

KEY WORDS

Penetrator Defect
Pipe Manufacturing
Resistance Welding
Oxide Inclusions
Paschen Discharge

J.-H. CHOI, Y. S. CHANG, and Y.-S. KIM are with the Department of Materials Science and Engineering, Hongik University, Seoul, Korea. C.-M. KIM is with POSCO Research Center, Pohang, Korea. J.-S. OH is with SeAh Steel Co. Ltd., currently Hanbee Setron, Pohang, Korea.

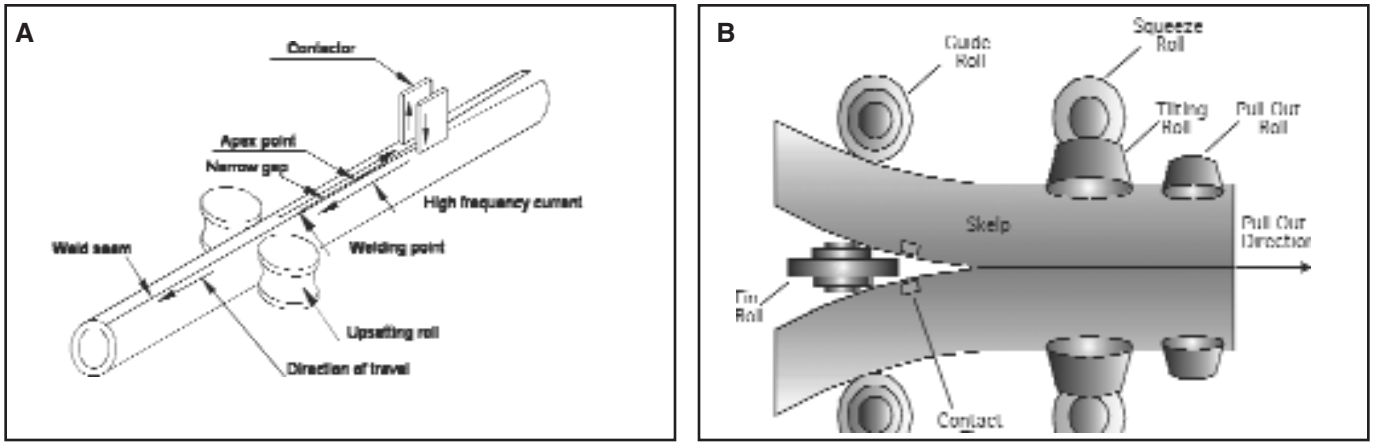

Fig. 1 — Schematic illustration of high-frequency electric resistance welding process: A — pipe mill; B — ERW simulator.

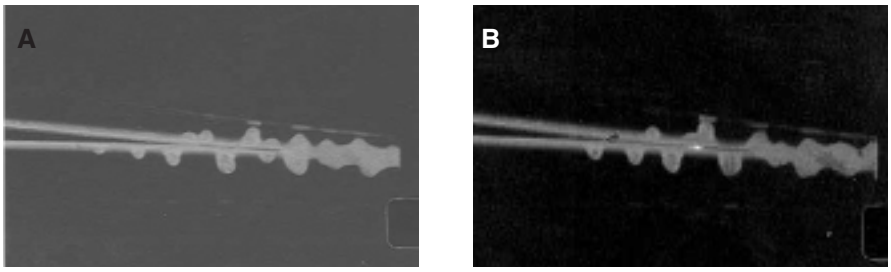

Fig. 2 — Typical melting behavior of strip edges during HF ERW: A — without polarization filter; B — with polarization filter.

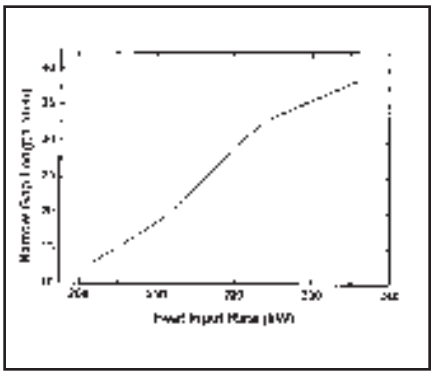

Fig. 3 — Narrow gap length as a function of heat input power. Welding speed was 18 m/min and strip thickness was 9.5 mm.

mm. Chemical composition of the strip was Fe-0.174C-0.109Si-0.837Mn-0.017P-0.007S-0.029Cu-0.03Ni-0.032Cr-0.019Al in wt-%. Heat input power was changed from 201 to 237 kW. The frequency of the current was 400 kHz. The welding phenomena were observed using a high-speed camera (Photonic Systems, Inc., Wayne, N.J.) and a high-speed video camera (NAC Inc., Tokyo). The framing rate was varied from 1000 to 10,000 pictures per second (pps) with the high-speed camera and from 1000 to 2000 pps with the video camera. In order to enhance the observation of the flashing at the apex point, neutral density, red color, and polarization filters were attached to the camera lenses. The ERW simulator was used to investigate the welding phenomena observed with the pipe mill in more detail, and its setup is shown schematically in Fig. 1B. The simulator does not have the forming section of pipe mills and joins two strips with a contact-type HF electric resistance welding machine.

In order to measure the area fraction of weld defects, the top surface of the sample was machined by one-fourth of the strip thickness followed by micropolishing. The length of each sample was 5 cm, and the total length of sample examined was 60 cm for each welding condition. The weld defect sizes and number were measured using optical microscopy combined with an image analyzer. More detailed analyses for the weld interface microstructure were made by scanning electron microscope (SEM) (Hitachi, Japan) with energy dispersive spectroscopy (EDS) (Kevex, U.S.).

Results and Discussion

Flashing and Bridge Formation

Figure 2 shows a high-speed cinematographic image of strip edges observed with and without a polarization filter during the HF ERW process. The edges melted well ahead of the welding point and the molten metal was driven out from the surface of the strip edges. Near the welding point, the narrow gap was developed as indicated by Haga et al. (Refs. 3, 4). The length of the gap was measured from images of the high-speed cinematography as a function of heat input power — Fig. 3. The narrow gap length increased linearly from 12 to 40 mm as the heat input power was changed from 201 to 237 kW.

When the melting behavior of the edges was observed with a polarization filter (Fig. 2B), flashes (which appear as white spots in the figure) that were not perceptible without the filter were observed to occur consistently throughout the whole range of heat input power investigated in this study. The frequency of flashing was in a range 0.1 to 5 kHz and varied depending on the heat input power. At low heat input powers, the frequency was relatively high and decreased with the heat input power.

One of the interesting phenomena to note from the flashing is the formation of a molten metal bridge between the edges. Just after the flashing, a molten metal bridge between the strip edges was formed and started to travel along the narrow gap. Figure 4 shows sequential images of the flashing and bridge movement during the HF ERW process. The images were filmed at a rate of 1000 pps using the high-speed video system. As shown in the figure, after the flashing near the apex point (one frame later, i.e., after 1 ms (Fig. 4B), a bridge between the two edges of the strip was formed. The bridge was observed to always travel toward the welding point. As the bridge traveled along the narrow gap, molten metal on the strip edge was swept to the welding point. Again, the sweeping action of the bridge along the narrow gap

occurred throughout the whole range of the heat input power investigated in this study, but differed in its frequency and distance depending on the rate.

The travel speed of the bridges was estimated by measuring the elapsed time to travel the narrow gap as a function of heat input power (Fig. 5). As the heat input power was increased from 201 to 237 kW, its speed increased from 160 to 375 m/min, peaking at an intermediate heat input power. The speed of the bridges is an order of magnitude faster than the traveling speed of the strip. Since the bridges travel at such high speeds, violent ripples of molten beads resulted when they reached the welding point. These observations indicate that not only the repulsive electromagnetic force but also the sweeping action of the bridge drive the molten metal out and away from the narrow gap, providing an oxide-free surface for forge welding. Figure 6 shows the distance of the sweeping motion of the bridges as a function of heat input power. The distance was approximately 8.6 mm when the heat input power was 201 kW. As the heat input power was increased to 237 kW, the distance was increased monotonically to 26.5 mm.

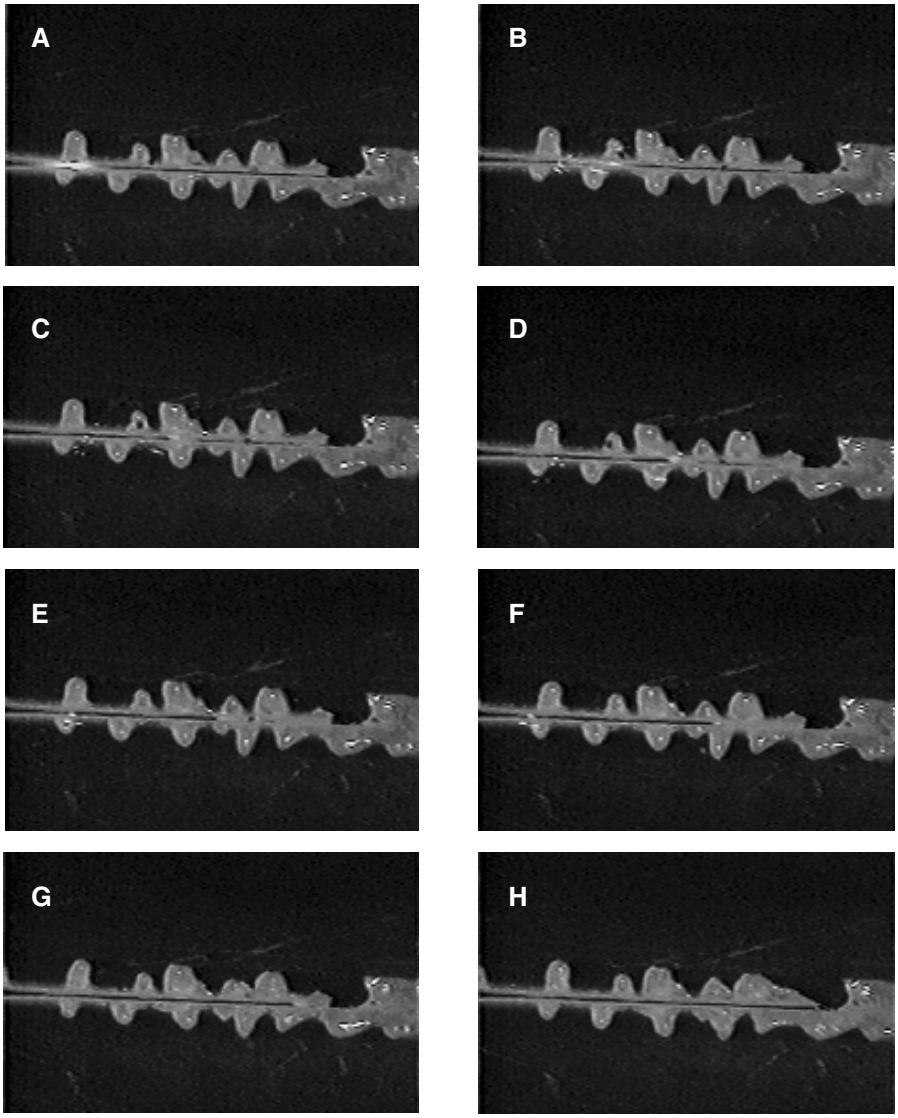

Fig. 4 — Sequential images of flashing and bridge movement during HF ERW: A — 0 ms; B — 1 ms; C — 2 ms; D — 3 ms; E — 4 ms; F — 5 ms; G — 8 ms; H — 12 ms.

Mechanism of Flashing and Bridge Movement during HF ERW

The flashing near the apex point and traveling of molten metal bridges along the narrow gap noted in this study are expected to have a significant influence on defect formation during the HF ERW process. The flashing occurred mainly in two different forms: one with a strong flash followed by expulsion of a molten metal bridge, and the other with a soft flash followed by the formation and movement of the bridge. The former flashing occurred infrequently and was observed mostly when protrusions on the strip edges, such as metal particles, short-circuit the edges. This type of flashing was irregular in frequency and was not affected by the welding conditions. The latter was observed to occur prior to the short circuit between the edges, and its frequency was affected by the welding conditions.

Flashing or discharging between two freestanding electrodes, i.e., between two strip edges in this case, could occur via Paschen discharge phenomenon, of which breakdown voltage, V_f, is given by Equation 1 (Ref. 10).

$$V_f = B \frac{pd}{k + \log pd} \qquad (1)$$

where p is the pressure of the discharging atmosphere, d is the distance between electrodes, and B and k are constants. Plotting of Equation 1 as a function of pd results in a skewed U-shaped curve. The minimum breakdown voltage of a system is affected by the frequency of current and ionization potential of the gas in the atmosphere (Ref. 11). High-frequency current and gaseous elements with lower ionization potential, such as metal atoms, decrease the breakdown voltage. For example, the discharge occurs at approximately 130 V when the electrode gap is 60 μm under Ne-Xe gas atmosphere with 50-kHz current (Ref. 12). In the HF ERW process, the breakdown voltage might be decreased further as the atmosphere contains species, such as Fe vapor, that have lower ionization potential, causing metallic arc discharge. The flashing observed in this study, therefore, seems to be caused by the Paschen discharge between the two freestanding strip edges in the narrow gap, where the electric field is the largest. The voltage applied between the strips during the HF ERW process was between 70 and 120 V.

Upon the flashing between strip edges, a significant fraction of welding current might be diverted through the discharge column, decreasing the electromagnetic pinch force on the liquid metal on the strip edges. Under this condition, molten metal on the narrow gap may fluctuate due to the sudden change of the pinch pressure and that should increase the possibility of bridge formation. In addition, uneven pressure distribution near the discharge column might have also promoted the formation of the bridge.

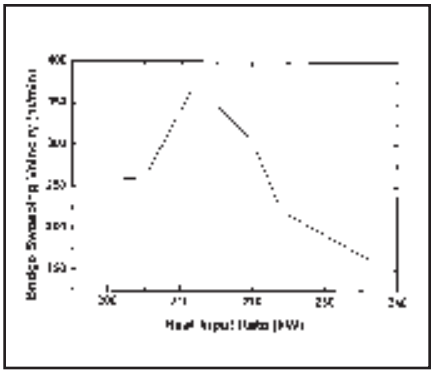

Fig. 5 — Sweeping speed of bridge as a function of heat input power.

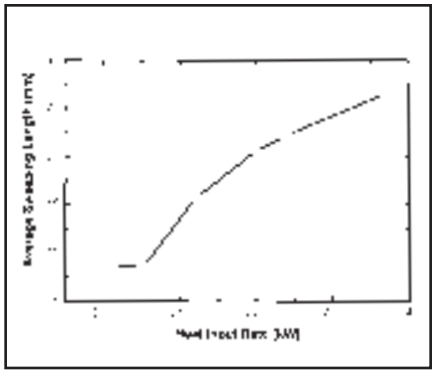

Fig. 6 — Sweeping distance of bridges as a function of heat input power.

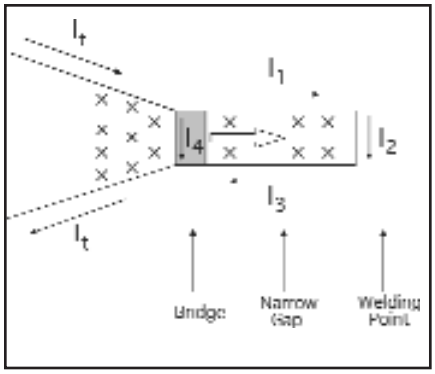

Fig. 7 — Schematic illustration of magnetic flux density distribution around a bridge.

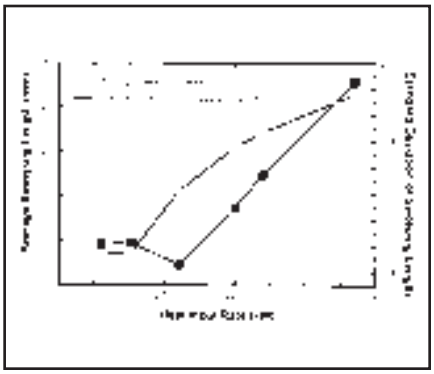

Fig. 8 — Sweeping length and standard deviation of bridge traveling along narrow gap measured as a function of heat input power.

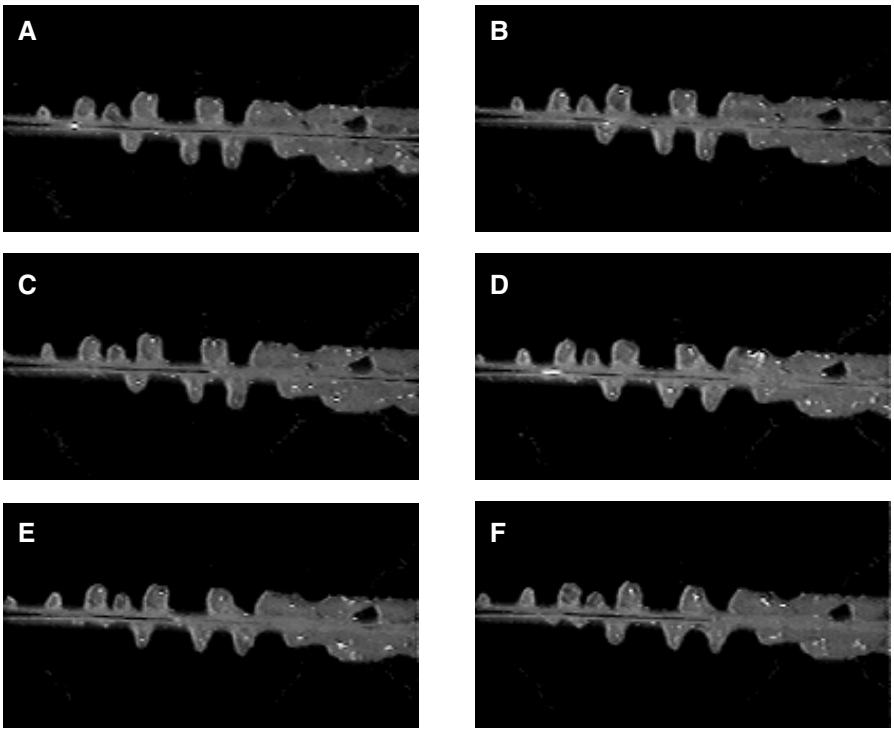

Fig. 9 — Stoppage of bridge movement and refilling of molten metal into narrow gap by multiple flashing. A — 0 ms; B — 2 ms; C — 5 ms; D — 9 ms; E — 12 ms; F — 15 ms.

Once the bridge was formed after the flashing, it always traveled toward the welding point at an order of magnitude faster than the strip, suggesting the presence of an external driving force for the movement. If a significant fraction of welding current is diverted to the bridge, the magnetic fluxes due to the currents flowing in strip edges and in the bridge have the same direction in the left-hand side of the bridge, but they are opposite in the narrow gap, as illustrated in Fig. 7. Since the electromagnetic pinch force on the bridge is given by the vector product of current density in the bridge and magnetic flux, the pinch force on the left-hand side of the bridge should be greater than that on the right-hand side of the bridge. This unbalanced pinch force seems to provide the driving force for the bridge movement toward the welding point. A numerical analysis of the electromagnetic field around the bridge in a further study is warranted, to justify the driving force for the bridge movement at the observed speed.

Relationship between Bridge Movement and Weld Defect in HF ERW

Since the bridge sweeps the molten metal containing oxides out of the narrow gap and faying interface, incomplete sweepings should lead to inclusions of oxide particles in the weldment. Figure 8 shows the standard deviation of the traveling distance along with the bridge travel distance. At low heat input powers, the deviation value was small; i.e., once the bridge is formed, it sweeps through the entire length of the narrow gap to the welding point. As the heat input power was increased, the deviation increased. In other words, a significant fraction of the bridges are stopped somewhere along the narrow gap and do not reach the welding point. This stoppage of the bridge movement was observed to be induced by the multiple bridges traveling along the narrow gap — Fig. 9. While the bridge formed from the first flashing traveled along the gap (Fig. 9B–D), a new bridge was formed by the second flashing (Fig. 9D) and started to travel (Fig. 9E). The formation of the second bridge should homogenize the electromagnetic field around the first bridge and result in the reduction in traveling speed, eventually stopping the bridge movement. The reduced travel speed of the bridge at higher heat input powers in Fig. 3 was observed to be related to the multiple bridges formed in the narrow gap. When the bridge was stopped on

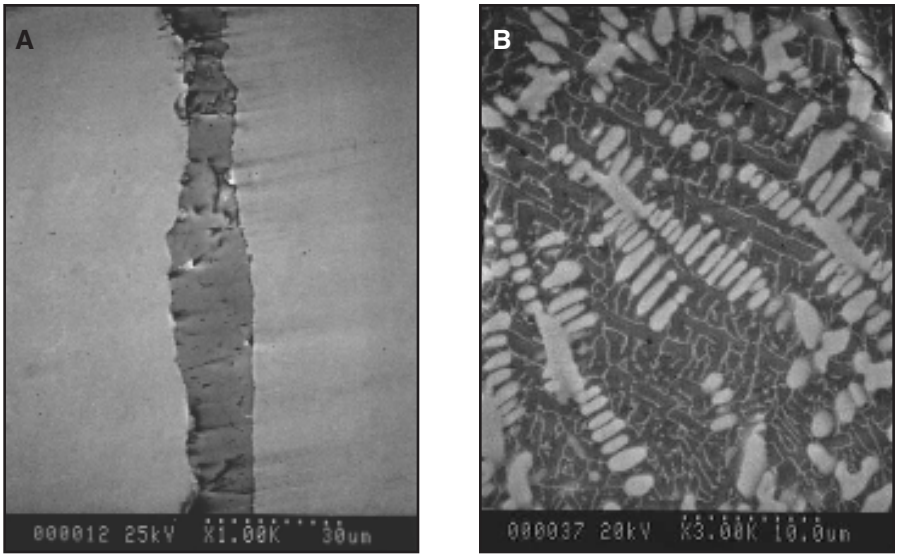

Fig. 10 — SEM micrographs of penetrator: A — formed at weldment; B — its microstructure at higher magnification.

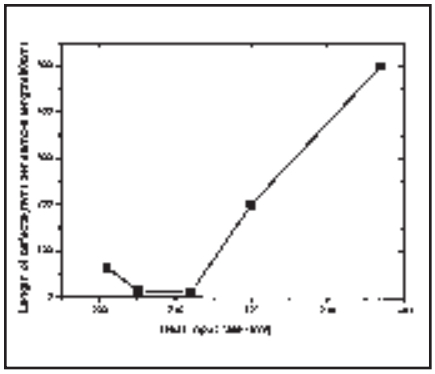

Fig. 11 — Effect of heat input power on the area fraction of oxide inclusions in weld.

the way to the welding point, the narrow gap between the bridge and the welding point was backfilled with the molten metal driven out from the narrow gap — Fig. 9F. The backfilling occurred very rapidly, in less than 2–5 ms.

Figure 10 shows a SEM micrograph of the penetrator formed at the weldment. The thickness of the defect was approximately 10 µm. Observation of the microstructure at a higher magnification indicated that the defect consisted of dendrites, typically observed in solidified materials. This result also provides experimental evidence that the penetrator is formed from backfilled molten metal.

Figure 11 shows a relationship between heat input power and fraction of oxide inclusions in welds. When compared with Fig. 8, the lowest defect density was noted when the standard deviation of the bridge movement was at a minimum. These results indicate that the weld defect density in welds of the HF ERW process is strongly affected by the regularity of the sweeping action of the bridge. The backfilling of the molten metal into the narrow gap caused by the irregular sweeping action seems to be the main reason for the formation of the penetrator defect in welds of the HF ERW process.

Conclusions

Welding phenomena during the HF ERW process were investigated using high-speed photographic techniques. The results indicated that flashing between strip edges occurs near the apex point at a frequency ranging from 0.1 to 5 kHz in every welding condition investigated. The flashing resulted in formation of a molten metal bridge, which always traveled toward the welding point at a speed ranging from 160 to 375 m/min. The movement, which may be caused by asymmetric distribution of the electromagnetic field around the bridge, swept molten metal mixed with oxides from the narrow gap.

When the bridge swept completely across the whole length of the narrow gap, the weld contained fewer weld defects. At higher welding heat input powers, sweeping action of the bridge became irregular and led to backfilling of molten metal into the narrow gap. At these conditions, the density of the weld defect, especially the oxide inclusion, increased. The refilling of the molten metal into the narrow gap caused by the irregular sweeping action seems to be the main reason for the formation of the penetrator defect in HF ERW welds.

References

1. Saito, M., Kasahara, H., Tominaga, H., and Watanabe, S. 1986. Theoretical analysis of current distribution in electrical resistance welding. *Transactions of ISIJ* 26:461–467.

2. Zinn, S., Semiatin, S. L., Harry, I. L., and Jeffress, R. D. 1988. *Elements of Induction Heating.* ASM International Publishing.

3. Watanabe, N., Funaki, M., Sanmiya, S., Kosuge, N., Haga, H., and Mizuhashi, N. 1986. An automatic power input control system in high-frequency electric resistance welding. *Transactions of ISIJ* 26:453–460.

4. Kyogoku, T., Takamadate, C., Hotta, K., Tatsuwaki, M., and Nemoto, S. 1983. Automatic welding control system of electric resistance weld tube mill. *Sumitomo Kinzzoku* 35(2): 61–73.

5. Choi, J.-H., Kim, C.-M., Yoo, C.-D., and Kim, Y.-S. 1999. Mechanisms of weld defect formation in HF ERW process. *Proceedings of International Conference on Tube Making for Asia's Recovery,* pp. 1–8. London, U.K.: International Tube Association.

6. Haga, H., Aoki, K., and Sato, T. 1980. Welding phenomena and welding mechanisms in high-frequency electric resistance welding — 1st report. *Welding Journal* 59(7): 208-s to 216-s.

7. Haga, H., Aoki, K., and Sato, T. 1981. The mechanisms of formation of weld defects in high-frequency electric resistance welding. *Welding Journal* 60(6): 104-s to 109-s.

8. Ichihara, H., Sumimoto, D., Kimura, T., Kimiya, Y., and Yoshizawa, M. 1986. Manufacture of alloy steel tube by high-frequency electric resistance welding. *Transactions of ISIJ* 26:468–475.

9. Snamiya. S., Miyata, S., Miyagawa, T., and Haga, H. 1989. New system for automatic heat input control according to SPL for ERW. *Sei Tetsu Keng Ku* 335:43–50.

10. Lieberman, M. A., and Lichtenberg, A. J. 1994. *Principles of Plasma Discharges and Materials Processing.* New York, N.Y.: John Wiley & Sons.

11. Chapman, B. 1980. *Glow Discharge Processes.* New York, N.Y.: John Wiley & Sons.

12. Oversluizen, G., Zwart, S., Dekker, T., Juestel, T., and van Heusden, S. 2002. Characteristics of a high-Xe-concentration in 4-in. PDP. *Journal of the SID* 10(3): 237–240.

Change of Address?

Moving?

Make sure delivery of your *Welding Journal* is not interrupted. Contact the Membership Department with your new address information — (800) 443-9353, ext. 480; *jleon@aws.org*.